Exploring the Effects of Pre-Existing Target Faults on Crater Morphology

Catherine S. Plesko, Applied Physics Theoretical Design Division, Los Alamos National Laboratory

Pre-existing inhomogeneities in the target geology are known to affect the formation and final geometry of an impact crater. Large joints appear to have caused the squaring off of Meteor Crater, and polygonal craters on Mars appear to track ring faults around the Hellas and Isidis impact basins [1]. Other examples have been seen on Venus [2] and the moon [3]. Here I present a numerical modeling exploration of the effects of pre-existing target faults on impact crater morphology.

Introduction

The impact cratering process places the target material under both compression and tension. The target is likely to have a spatially inhomogeneous strength before the time of impact. Joints, faults and other inhomogeneities can affect the geometry of the final crater. Further shock damage to the target during the cratering process can affect the final crater geometry, such as in the case of complex craters, and post-impact fault slip can also affect crater morphology. One of the peculiarities of Meteor Crater in Arizona is its unusual squared shape that is thought to be caused by the presence of orthogonal joints in the target rock that cut vertically through the host rock and intersect at the point of impact [4], which opened as angular tear faults on the crater rim either during the excavation [5] or modification [6] phase. The joints at Meteor Crater are of order a meter wide or less. Fault zones generally can be much wider in areas where the host rock has been damaged by fault slip.

Models

The models are 3-D cartesian models of an impact similar to that which made Meteor Crater [7]. The impactor is 50 m in diameter and strikes a layered sandstone and limestone target at a 45-degree incidence with an impact velocity of 12.5 km/s. I approximate a fault zone or joint in these models with vertical inclusions of strengthless, lower density rock, in this case, Nevada Alluvium. The thickness of the fault zone is variable, shown at $t = 0$ in Fig. 1.

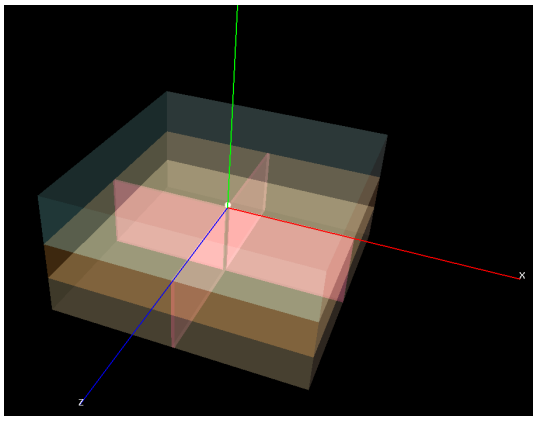

Figure 1: Initial conditions of an example mesh. The target is air over limestone over sandstone with a 50-km-diameter iron impactor striking at 12.5 km/s and 45-degrees at the intersection of two perpendicular 50-meter-thick fault zones.

I explore the effects of pre-existing target flaws on the excavation process using the RAGE and FLAG hydrocodes, and the effects of fault slip late/modification stage using the Abaqus finite element analysis (FEA) suite. Finite element analysis techniques are more appropriate than hydrocodes to analyze scenarios where the motion of particles and pressure waves remain well below the sound speed of the medium in question. Abaqus is a standard tool used in many industries from aerospace engineering to mining. The radiation grid Eulerian (RAGE) code [8], [9] is a compressive Eulerian hydrocode with radiative transfer enabled. It uses continuous adaptive mesh refinement (CAMR) for increased accuracy and computational efficiency. Simulations may be carried out in one, two, or three dimensions, and in Cartesian, cylindrical, or spherical coordinate systems. Elastic-Plastic and Steinberg-Guinan strength models, and a P-α crush model are included for modeling of solids. I chose

to use RAGE for its ease of use in rapid simulation setup and efficacy in the gravity regime. I am running additional models in the Free Lagrangian (FLAG) hydrocode, described in [10]. FLAG is a well-validated Lagrangian/ALE hydrocode developed and maintained by the Lagrangian Applications project at LANL. I chose to use it because it has a greater range of solid mechanics options available to it than RAGE does, given the relative ease of implementation of solid mechanics in Lagrangian over Eulerian numerical schemes. Both codes use the LANL SESAME material property database [11] for equations of state. I used the OSO computational geometry design software to set up the initial meshes for all three sets of models. The RAGE and FLAG meshes are identical at $t = 0$, but refine according to their respective CAMR and ALE schemes, which I try to keep as similar as possible. The post-impact Abaqus models uses a similar setup, but with a hemispherical crater assumed at the intersection of the two joints in the target.

Preliminary Results

Initial calculations use a fault zone that is 50 times wider than the joints seen at Meteor Crater. The transient crater, shown in Fig. 2 from the RAGE model at $t = 10.0$ seconds, approximately the time of transition to the modification stage is slightly squared off, but the corners are 90 degrees off from those seen at Meteor Crater. The thick fault zone appears to flatten the rim as it expands along the fault zone. Calculations using fault zones of thicknesses $dx = 50, 25, 10$, and 1m are ongoing, and further results will be presented at the meeting. If the final squaring off of the crater along the fault lines happens through slumping during the modification stage as predicted by Poelchau et al. [6], it is likely that the FEA models will be the most informative of this suite. If it happens during excavation, the hydrocode models should be the most indicative, but are sensitive to the resolution and physical parameters assumed for the fault zone.

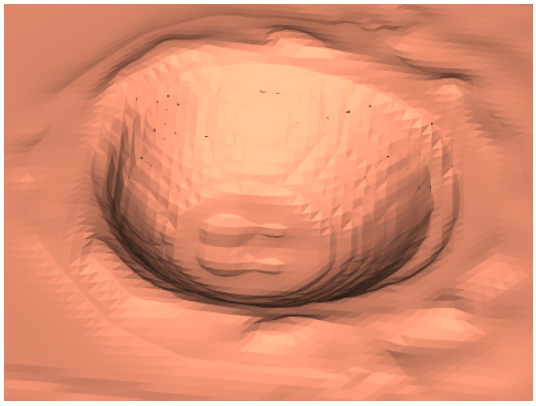

Figure 2: RAGE model at $t = 10.0$ seeconds, isosurface of density at $rho = 2.4$ g/cm^3. The crater is squared, but the corners are 90 degrees off from the final rim at Meteor Crater. The thicker $dx = 50$m fault zone appears to flatten the rim as it expands.

References

[1] Oehman, T., Aittola, M., Kostama, V.-P., and Raitala, J. In *Impact Tectonics*. Springer (2005). [2] Aittola, M. T., Ohman, T., Leitner, J. J., and Raitala, J. *Earth Moon and Planets* **101** (2007). [3] Eppler, D. T., Ehrlich, R., Nummedal, D., and Schultz, P. H. *Geol. Soc. Am. Bull.* **94** (1983). [4] Gault, D. E., Quaide, W. I., and Oberbeck, V. R. *Shock metamorphism of natural materials*, chapter Impact cratering mechanics and structures, 87–100. Mono Book Corps. (1968). [5] Roddy, D. J. *Proceedings of the ... Lunar and Planetary Science Conference* (1978). [6] Poelchau, M. H., Kenkmann, T., and Kring, D. A. *J. of Geophys. Res.* **114**(E01006) (2009). [7] Kring, D. A. *Guidebook to the Geology of Barringer Meteorite Crater, Arizona (a.k.a. Meteor Crater)*. LPI Contribution 1355. Lunar and Planetary Institute, (2007). [8] et al., G. M. L. *Computational Science and Discovery* **1**(1) October (2008). [9] Pierazzo, E. and et al. *LPI Contributions* **1423**, 3022–+ (2008). [10] Burton, D. E. In *Advances in the Free Lagrange Method*. Springer-Verlag, New York (1990). [11] Johnson, J. D. In *Proc.12th Symposium on Thermophysical Properties*. Los Alamos National Laboratory, June (1994). LA-UR-94-1451.